Mapping the Ejecta in the Peculiar SNR 3C397

E. Franzmann & S. Safi-Harb
(University of Manitoba, Canada)

Abstract:

The SNR 3C397 has a peculiar morphology with a central X-ray `hot spot' and a sharp boundary in the west. Earlier studies showed that the column density increases from east to west and that the X-ray spectrum is dominated by thermal emission from (at least) two components: a low-temperature plasma with a high ionization timescale, mixed with a high-temperature, ejecta-dominated plasma (mainly Fe-K), with a low ionization timescale. This, together with millimeter observations of the environs of 3C 397, suggests that 3C 397 is a ~5 kyr old SNR, encountering a molecular cloud towards the west, and evolving into a mixed-morphology SNR. We present an analysis of 3C 397 with Chandra and XMM-Newton targeted to map the ejecta distribution and thus shed light on the nature of the progenitor star.

Introduction

•3C 397 makes an interesting object for study, partly due to its unusual, highly asymmetric, box-like morphology.
•Some previous findings:
- High resolution radio imaging (Becker et al. 1985; Anderson & Rudnick 1993) find that the remnant brightens on the edge closest to the Galactic plane
- In radio, the SNR has the appearance of a "shell" and has been therefore classified as shell type (Green, 2004).
- Anderson & Rudnick (1993) also found variations in the radio spectral index across the SNR and attributed it to interactions between the expanding SNR and surrounding medium.
- Dyer & Reynolds (1999) found the same magnitude of variations, but did not confirm detailed spacial findings.
- ROSAT observations (Rho 1995; Rho & Petre 1998; Dyer & Reynolds 1999; Chen et al. 1999; Safi-Harb et al. 2000) find 2'.5 x 4'.5 diffuse emission with enhancement in both central emission (referred to as the "hot spot") and on the western side of the SNR.
- Safi-Harb et al. (2000) find the overall X-ray spectrum to be heavily absorbed, complex and dominated by thermal emission from ejecta and an ISM component.
- Neutral Hydrogen absorption measurements put the SNR between 6.4-12.8 kpc (Caswell et al. 1975).
- At a distance of 10 kpc, the linear size of the radio shell would be 7 x 13 pc

•From the Chandra and multi-wavelength imaging study (Safi-Harb et al. 2005) we know that:
- (At least) 2-component models are required to adequately account for the X-ray emission from the SNR, even from small (arcseconds)-scale regions across the SNR.
- A 2-component VPSHOCK model provided adequate fits to various regions across the remnant, and showed the following trends:
  - Column density increases from east to west, indicating the presence of a denser medium in the west.
  - Soft component temperature varies between ~0.15-0.26 keV with a high ionization timescale and (generally) solar abundances.
  - Hard component temperature varies between ~1-3 keV with ionization timescales that were generally lower than the soft component, and usually requiring above-solar S and Fe abundances (even in outer regions), indicating the presence of hot ejecta.
- Multi-wavelength imaging and spectral properties point towards 3C397 being a young ~5300-year old SNR propagating in a medium with a density gradient, encountering a molecular cloud to the west (supported by mm observations), and evolving into a mixed morphology SNR (see Rho & Petre 1998 for more information on mixed morphology SNRs)
- Recent CO observations (Jiang et al.) show that the remnant is confined in a cavity of molecular gas and confirm that it's embedded at the edge of a molecular cloud.

XMM-Newton Observations

•This project used EPIC data from 3 separate observations of 3C 397. The object was observed on October 15, 2003 (Obs ID 0085200301, set 1) and April 23, (0085200401, set 2) and 25, 2004 (0085200501, set 3)
•We used the Science Analysis System (SAS, version 7.1) for data reduction and image creation. Further processing on the line images was performed using ImageJ and ds9.
•All images were produced from event lists filtered to only include approved patterns (pattern ≤ 12 for MOS, ≤ 4 for PN) and good time intervals. GTI filtering was achieved using light curves between 10-12 keV. Spectra were additionally filtered using FLAG = 0 for all cameras (and all data sets).
•The duration of the exposures after filtering each event list is: 15 ks for each MOS and 8 ks for the PN in set 1; 16 ks (each MOS) and 11 ks (PN) in set 2; and 11 ks (each MOS) and 5 ks (PN) in set 3.
• The primary goal of our present study is to map and isolate the ejecta in the SNR.
•XMM's large effective area and good angular and spectral resolution in the 0.2-10 keV band make it ideal for this study.

Imaging

XMM Broadband & 4-6 keV Continuum Images

•Figure 1 shows both the 0.5-10 keV and 4-6 keV images with VLA L-band contours overlaid.
•The 0.5-10 keV image has been smoothed with a ~4" Gaussian blurr, while the 4-6 keV image (line-free region) has been smoothed with a ~7" Gaussian blurr.

Line Images

As with previous X-ray studies, the emission from the SNR is dominated by thermal emission, in particular from Mg, Si, S, and Fe-K. Line images of these elements were then made using the method outlined in Cassam-Chenaï et al. (2004), and is summarized as follows:
•To make the line images, the background-subtracted spectrum in the line region (in counts/keV) was fit to a Gaussian plus a simple continuum model (power law or exponential) in order to estimate the shape of the continuum under the line.

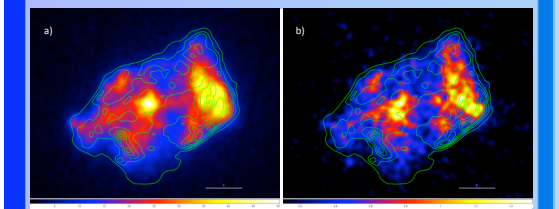

Figure 1 – **a)** 0.5-10 keV broadband image, smoothed by ~4" Gaussian, and **b)** 4-6 keV ("line-free") continuum emission, smoothed by ~7" Gaussian. Both images have the VLA L-Band contours overlaid in green. The white bar in the images corresponds to a scale of 1'.

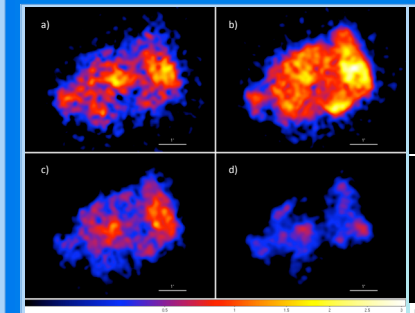

Figure 2 – Individual background and continuum subtracted line images, with each being respectively **a)** Mg, **b)** Si, **c)** S and **d)** Fe. All images are displayed with square root scaling, with the same minimum and maximum limits as displayed by the colour bar. The white line near the bottom of each limits represents 1'.

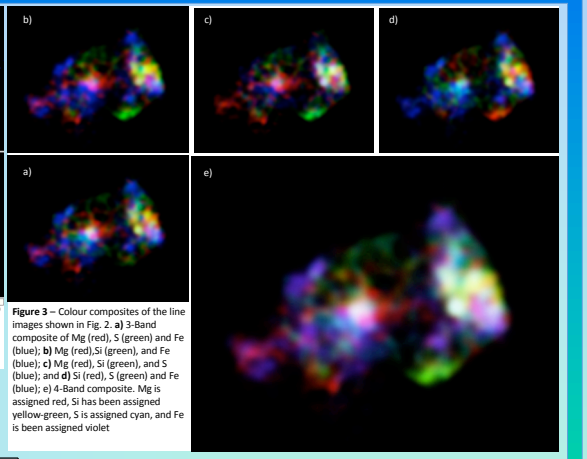

Figure 3 – Colour composites of the line images shown in Fig. 2. **a)** 3-Band composite of Mg (red), S (green) and Fe (blue); **b)** Mg (red),Si (green), and Fe (blue); **c)** Mg (red), Si (green), and S (blue); and **d)** Si (red), S (green) and Fe (blue); e) 4-Band composite. Mg is assigned red, Si has been assigned yellow-green, S is assigned cyan, and Fe is been assigned violet

- To determine the optimal line extraction band, the Signal-to-Noise ratio of the model spectrum was optimized.
- Line images, along with two continuum side-bands, were extracted at the following energies:

Line:	Line Band:	Continuum⁻:	Continuum⁺:
Mg	1.29-1.40 keV	1.10-1.24 keV	1.45-1.60 keV
Si	1.78-1.92 keV	1.54-1.72 keV	1.98-2.10 keV
S	2.38-2.54 keV	2.26-2.31 keV	2.60-2.80 keV
Fe	6.32-6.84 keV	4.20-6.16 keV	7.00-7.40 keV

- To estimate the underlying continuum, the two continuum side-band images were measured and scaled, so that the number of background-subtracted image counts in the spectral extraction region matched the number of counts predicted from integrating the continuum model in the line band.
- To create the continuum images, a linear interpolation of the scaled continuum images was taken:

$$I_c(i,j) = \lambda\alpha_c^- I_c^-(i,j) + (1-\lambda)\alpha_c^+ I_c^+(i,j)$$

where the α's are the scaling constants, and λ is a weighting factor between 0-1.
- The continuum image was then subtracted from the corresponding (background-subtracted) line-band image to create an image of the emission from the line.
- Both the Line-band and estimated continuum images were smoothed by a ~10" radius Gaussian prior to image subtraction. Figure 3 displays each line image at identical square root scaling.

Line Image Colour Composites

- Each line image has been normalized by its maximum value and contrast enhanced to emphasize its brightest regions prior to colour compositing.

4-Band Image
- This was created to try and identify features common to all elements as well as map the distribution of all 4 elements across the SNR.
- In this image (Figure 3e), the Mg image has been coloured red, the Si image has been coloured yellow-green (half-way between red and cyan), the S image has been coloured cyan, and the Fe image has been coloured violet (colour compliment to Si image). The image has been further contrast enhanced to bring out more detail.

3-Band Images
- The 3-Band images were made to help try and identify individual features that may be washed out in the 4-Band image.
- Each of these images contain 3 of the four lines, contrast enhanced in the same way as the 4-colour image. Images are coloured red (softest line), green, and blue (hardest line). (Figure 3, a) displays Mg, S, and Fe, (b) displays Mg, Si and, Fe, (c) displays Mg, Si, and S, and (d) displays Si, S, and Fe.

Equivalent Width (EQW) Images

•Each EQW image is created by dividing each background- and continuum-subtracted line image by its corresponding continuum image.
•Due to the fact that the background noise is amplified, a mask, made by thresholding each line image to remove the surrounding background, has been applied to each image to remove the background around the remnant.
•Figure 4 displays each EQW image with the contours from its corresponding line image overlaid.

3-Band Image

•The 3-band image (Figure 5) is a colour composite image of the 0.5-1.5 (assigned red), 1.5-2.5 (green), and 2.5-8.0 keV (blue) bands. Each image has been smoothed by a Gaussian kernel with a radius of ~7", then normalized by its maximum value before compositing. The resulting image has been contrast enhanced to better display the differences in the bands.

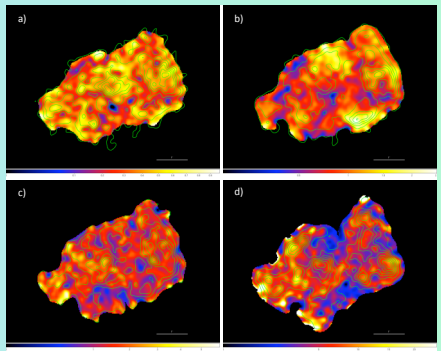

Figure 4 – **a)** Mg, **b)** Si, **c)** S and **d)** Fe equivalent width images displayed with square root scaling an with corresponding line image contours overlaid in green. The white bar near the bottom of each image represents 1'

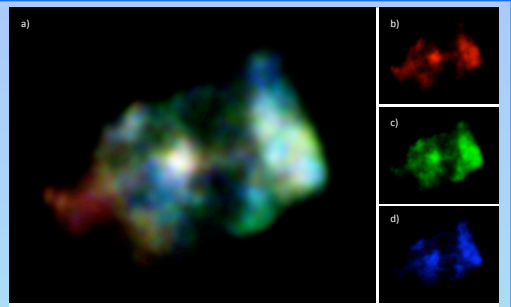

Figure 5 – **a)** colour composite of images of the 0.5-1.5 (red, **b**), 1.5-2.5 (green, **c**), and 2.5-8 keV (blue, **d**) bands. Each image has been blurred by a ~7" Gaussian kernel, then normalized by its maximum pixel value prior to colour compositing.

Discussion

•The eastern part of remnant appears to be dominated by softer X-ray emission – note the soft plume (tail-like) structure highlighted in "red" in Figure 5 (a), showing relatively harder emission towards the centre and west.
•There is clearly a faint ridge of emission between the SNR's center and the western lobe. This curious region is apparently void of all the elements, except for a very faint soft jet-like structure along the east-west axis connecting the hot spot with the western region.
•The line images (Fig. 2) show that overall the Mg and Si line emission is brighter and more extended, whereas the S and particularly Fe emission is faint and appear more localized within the SNR shell.
•Overall the western region and the central "hot spot" appear to have more mixed emission from Mg, Si, S and Fe than the eastern region. This is evident from the white colour of the hot spot and the sharp boundary in the west (Fig. 4 e)).
•While all four line images show brightly in both the central spot and western lobe, Mg and Fe peak towards the center with some significant presence in the east, and Si and S peak in the western region.
•One particular structure, consisting of three knots in the western part of the SNR, shows prominently in Mg, Si and S (yellow in Fig. 3 a), b), and, d), and white in Fig. 3 c)).
•Si clearly has a prominent bright arc-like structure in the southwest (shown in green in Fig. 3 b), c), and e) and in red in Fig. 3 d)), seeming to be completely Si with a slight presence of S (not relatively very bright). This arc also appears to have a counterpart in the northwest. This counter-arc appears more prominent in the Si equivalent width image (Fig. 4 b)).
•Just above the bright Si arc (in the southwest) is a small knot that appears to be mostly Fe, also showing prominently in Fe are a couple small knots in the northeastern region of the remnant, above the central "hot spot".
•Fig. 3 d) shows very little magenta, which seems to indicate that the Fe knots (blue) in the western region contain very little Si (red). This also seems true across the remnant, except in the hot spot region.

Conclusions

We have presented a study of the SNR 3C 397 with XMM-Newton, in particular broadband, line-free, continuum-subtracted line images, and equivalent width maps with the primary goal to map and localize the ejecta of the supernova explosion. While Si, S, Mg and Fe appear mixed in many regions of the SNR, in particular in the central hot spot and the sharp western boundary, we have isolated some knots, in particular apparently pure Si and Fe knots. We will be next investigating the spectral properties of these localized regions.

Acknowledgements

This project was funded by the National Sciences and Engineering Research Council of Canada (NSERC) and the Canada Research Chairs program. Special thanks to Jason Fiege for his help in fitting the counts spectra, and to Steve Reynolds for providing us with the VLA image.

References

•Anderson, M. C., & Rudnick, L. 1993, ApJ, 408, 514
•Becker, R. H., Markert, T., & Donahue, M. 1985, ApJ, 296, 461
•Cassam-Chenaï, G., Decourchelle, A., Ballet, J., Hwang, U., Hughes, J. P., & Petre, R. 2004, A&A, 414, 545
•Caswell, J. L., Murray, J. D., Roger, R. S., Cole, D. J., & Cooke, D. J. 1975, A&A, 45, 239
•Chen, Y., Sun, M., Wang, Z.-R., & Yin, Q. F. 1999, ApJ, 520, 737
•Dyer, K. K. & Reynolds, S. P. 1999, ApJ, 526, 365
•Green, D. A. 2004, A Catalogue of Galactic Supernva Remnants (Cambridge: MRAO), http://www.mrao.cam.ac.uk/surveys/snrs
•Jiang, B., Chen, Y., Wang, J., Su, Y., Zhou, X., Safi-Harb, S., Delaney, T. 2009, submitted
•Rho, J. 1995, Ph.D. thesis, Univ. Maryland
•Rho, J., & Petre, R. 1997, ApJ, 484, 828
•Safi-Harb, S., Petre, R., Arnaud, K. A., Keohane, J. W., Borkowski, K. J., Dyer, K. K., Reynolds, S. P., & Hughes, J. P. 2000, ApJ, 545, 922
•Safi-Harb, S., Dubner, G., Petre, R., Holt, S. S., Durouchoux, P. 2005, ApJ, 618, 321